# FATIGUE CRACK PROPAGATION OF DISSIMILAR METAL WELDS

C.S. Kusko[1], J.N. DuPont[1], S. Spooner[2], and A.R. Marder[1]

1. Department of Materials Science and Engineering, Lehigh University, Bethlehem, PA 18015, USA
2. Oak Ridge National Laboratory, Oak Ridge, TN 37831, USA

## ABSTRACT

The hard martensite layer that forms adjacent to the fusion line of austenitic/ferritic dissimilar metal welds has been investigated by microstructural characterization and mechanical testing methods. Residual stress measurements were made in the vicinity of the fusion line in both the substrate and overlay materials and fatigue crack propagation tests were performed as to allow the crack to propagate along the dissimilar alloy weld fusion line. This hard martensite layer was found to be non-detrimental to the fatigue crack growth response, as the majority of the fatigue cracks propagated across the martensite layer and fusion line and into the substrate. The compressive residual stresses within the substrate contributed to the enhancement of the growth response of the weld overlay specimens. Based on these results, the hard martensite layer should not be a major factor in causing failure along the fusion line in austenitic/ferritic dissimilar metal weld overlay applications.

## KEY WORDS

fatigue crack propagation; microstructure; martensite; weld

## INTRODUCTION

In the power generation industry, austenitic weld overlays are often used for erosion and high temperature corrosion resistance for ferritic carbon and low alloy steels [1]. Fabrication of such dissimilar metal welds can result in distinct problems. For example, rapid cooling and overlay/substrate chemical composition differences [2] lead to the formation of a martensite layer adjacent to the weld fusion line [3-11]. Figure 1 illustrates a typical martensite layer that forms along the fusion line of a 309L stainless steel/A285 carbon steel weld [11]. Previous research by Kusko [11] has provided a fundamental explanation for the formation of the martensite layer, which leads to steep microstructural and mechanical property gradients across the fusion line. For example, Figure 2 illustrates microhardness results conducted across the fusion line of the 309L stainless steel/A285 carbon steel weld [12]. As evidenced from this figure, the hardness in the martensite layer region can reach values that are approximately twice as large as the hardness values found in the bulk austenitic overlay and ferritic substrate. In addition to this detrimental microstructural gradient, the coefficient of thermal expansion mismatch between the overlay and the base material induces thermal stresses at the fusion line [2]. A post-weld heat treatment (PWHT), which is often incorporated in order to reduce the magnitude of residual stresses, can induce significant microstructural changes and thus, additional gradients in mechanical properties [3].

It is generally known that fatigue crack initiation often occurs more rapidly in welded structures as compared to non-welded structures due to welding defects and other stress concentrators. Consequently, a significant portion of a weld's fatigue life is spent in the propagation stage. The presence of such weld-related stress concentrators, in addition to the aforementioned hard martensite layer found adjacent to the fusion line, makes fatigue crack propagation a concern for dissimilar metal welds. In addition, residual stresses resulting from welding and

thermal expansion mismatch in the vicinity of a weld can significantly affect the fatigue behavior. Thus, knowledge of the fatigue crack growth behavior of such welds is of practical importance.

The objectives of this research are to investigate the fatigue crack growth behavior in the presence of the martensite layer found adjacent to the fusion line for as-welded (AW) 309L stainless steel/A285 carbon steel dissimilar metal welds. Included in this objective is an understanding of the residual stress pattern that can develop in such dissimilar metal weld overlay coatings. The results of this research should provide insight as to whether the martensite layer in such dissimilar welds should be of concern in the presence of cyclic loading conditions during service.

## EXPERIMENTAL PROCEDURE

Carbon steel designation ASTM A285 Grade C, of dimensions 61 cm x 15 cm x 4 cm, was utilized as the substrate material. The austenitic overlay used was iron-based 309L stainless steel. The weld strip electrode size was 30 mm × 0.5 mm. Strip electrode and substrate compositions are provided in Table 1. Electroslag welding was used to deposit the strip electrode continuously along the top edge of the substrate at 565 A, 24 V, and 3.0 mm/s travel speed. The electroslag process was chosen because of its abilities to produce a relatively flat fusion line and to provide a uniform cladding with low dilution levels [8]. The resulting dilution level was 17 %.

Compact-tension (C(T)) specimens were fabricated from specimens comprised of bulk electroslag welds and electron-beam (EB) extensions of the overlay material. EB welding was chosen to produce a minimal heat affected zone, allowing the original dissimilar metal electroslag fusion line microstructure to remain unchanged during the process. The resulting C(T) specimens were of dimensions 63.5 mm x 60.96 mm x 12.7 mm. Starter notches having a 1.52 mm radius of curvature were inserted by wire electro-discharge machining (EDM) as close to the fusion line as possible as to enable crack growth along the fusion line (parallel to the welding direction). However, since the welding process resulted in a fusion line that was not perfectly flat, it was impossible to insert the starter notch perfectly along the fusion line. Figure 3 shows a photomacrograph of a typical C(T) specimen with starter notch.

Neutron diffraction measurements were utilized to determine the residual stress pattern in three orthogonal directions near the dissimilar alloy C(T) specimen weld fusion line. Measurements were performed on the 309L stainless steel AW specimens. Due to differences in crystal structure between the substrate and the overlay, the measurements could not be conducted directly on the fusion line. Thus, for each sample, strains were measured at distances of 1, 3, and 5 mm from the dissimilar alloy weld fusion line (into both the substrate and overlay) at the notch tip, 10 mm, and 20 mm from the notch tip, as illustrated in Figure 4.

Fatigue crack propagation tests, conforming to ASTM Standard E647 [13], were performed on AW specimens and on wrought 309L stainless steel and A285 specimens to provide a baseline. Instron servohydraulic fatigue testing equipment was utilized, along with constant amplitude loading and a sine waveform. All testing was performed at a frequency of 25 Hz. Software from Fracture Technology Associates was used to allow for computer-controlled testing. Constant R (equal to 0.10) tests were utilized to generate steady state and higher crack growth rate data. Constant $K_{max}$ tests, during which the R ratio increased as the load decreased, were utilized to obtain low crack growth rate and threshold data. Crack lengths were determined by the compliance function and visually verified. Crack growth rates were calculated by the modified secant method. Stereomicroscopy and light optical microscopy were used to characterize the fracture surface and microstructure of the welds following testing.

## RESULTS AND DISCUSSION

### *Residual Stress*

Figure 4 shows the residual stress measurements for the 309L stainless steel/A285 carbon steel dissimilar metal weld in the AW condition for the normal (N), transverse (T), and longitudinal (L) directions of the stress. In this figure, the x-axis represents the magnitude of the residual stress, with positive values corresponding to tensile stresses and negative values corresponding to compressive stresses. The y-axis exhibits the distance from the fusion line, with positive values corresponding to locations within the austenitic overlay and negative values corresponding to locations within the ferritic substrate. The legend key illustrates the measurements taken at the notch tip and at 10 mm and 20 mm from the notch tip. From this figure, the residual stresses are tensile in the

309L stainless steel overlay and compressive in the ferritic substrate. Within the overlay, the magnitude of the stresses generally increase as the measurement location increases in reference to the notch tip such that the stresses at the notch tip are generally the smallest in magnitude. The residual stresses reach a maximum value of approximately 560 MPa, but are generally on the order of magnitude of 400 MPa or less for this dissimilar metal weld. Within the substrate, the compressive residual stresses reach a maximum value of approximately 130 MPa.

***Fatigue Crack Propagation Testing***

Figure 5 shows the C(T) specimens for the 309L stainless steel/A285 carbon steel samples in the AW (5a and 5b) condition following fatigue crack propagation testing. As evidenced from Figure 5a, which corresponds to test identification 309DMW3, the crack grew nearly parallel to and along the fusion line for this specimen. However, Figure 5b, which corresponds to test identification 309DMW2, illustrates that the fatigue crack grew across the fusion line and into the substrate and remained in the substrate during propagation.

Figure 6 exhibits the interaction of the crack with the fusion line microstructure for test specimen 309DMW3 (corresponding to Figure 5a), which macroscopically followed the interface. As evidenced from this figure, the extremely hard martensite layer, shown by Figures 1 and 2, does not appear to detrimentally affect the fatigue behavior as might be expected from such a hard layer. That is, propagation does not occur within the martensite layer. The interaction of the fatigue crack with the martensite layer in Figure 6a is representative of only a localized region of the crack growth. Figure 6b, which exhibits the fatigue crack in a different region of the same specimen as in Figure 6a, is more indicative of the entire crack path, such that little interaction exists with the martensite layer.

Crack growth rates for the two 309L stainless steel welds, in addition to wrought 309L stainless steel and A285 specimens, are plotted in Figure 7. As evidenced from this figure, the dissimilar metal welds exhibit increased fatigue resistance as compared to the wrought stainless steel and carbon steel specimens. Crack growth into the substrate, which experiences compressive residual stresses, most likely contributes to the enhanced fatigue response. Even the specimen that propagated a small distance through the martensite layer exhibited an improved response, indicating a possible retardation of the fatigue response caused by the martensite layer. Regardless, the main point to emphasize is that, as evidenced by this figure, in conjunction with Figures 5 and 6, the martensite layer does not appear to detrimentally affect the fatigue crack growth behavior of these austenitic/ferritic dissimilar alloy welds.

## CONCLUSIONS

Residual stress measurements made within the vicinity of the fusion line for the dissimilar alloy welds indicated compressive behavior in the substrate and tensile behavior in the overlay. Fatigue crack propagation results indicated that crack growth either crossed over the martensite layer and fusion line and continued within the compressive substrate or continued in the vicinity of the martensite layer within the overlay. Regardless, the hard martensite layer did not negatively affect the fatigue response of the welded materials, as the cracks never propagated fully within the martensite layer. In addition, the crack growth rate curves for the weld overlay specimens exhibited increased fatigue crack propagation resistance as compared to the wrought specimens, most likely due to the compressive residual stresses within the substrate region in which the cracks propagated. Based on these results, the martensite layer does not appear to present a major concern for contributing to interfacial failure in weld overlay applications in austenitic/ferritic dissimilar metal welds.

## ACKNOWLEDGEMENTS

The authors would like to thank Dr. C. Robino at Sandia National Laboratories for the electron beam welding, A. Benscoter for assistance with sample metallurgical preparation, G. Kozma for assistance with the testing equipment, and M. Rex for assistance with specimen machining. This research was sponsored by the American Welding Society Navy Joining Center Fellowship and a consortium of power generation companies.

## REFERENCES

1. Nelson, T., Lippold, J., and Mills, M. (1998). *Science and Technology of Welding and Joining* 3, 249-255.

2. Wang, Z., Xu, B., and Cii, Y. (1993). *Welding Journal*. 72, 397s-402s.
3. Gittos, M. and Gooch, T. (1992). *Welding Journal*. 71, 461s-472s.
4. Ornath, F., Soudry, J., Weiss, B.Z., and Minkoff, I. (1981). *Welding Journal.* 60, 227s-231s.
5. Faber, G. and Gooch, T. (1982). *Welding in the World.* 20, 87-98.
6. Pan, C., Wang, R., Gui, J., and Shi, Y. (1990). *Journal of Materials Science.* 25, 3281-3285.
7. Pohle, C. (1991) *Welding International.* 5, 409-413.
8. Zhao, Q., Gao, Y., Devletian, J., McCarthy, J., and Wood, W. (1993). In: *International Trends in Welding Science and Technology*, pp. 339-343, David, S.A. and Vitek, J.M. (Eds). Gatlinburg, Tennessee.
9. Pan, C. and Zhang, Z. (1994). *Materials Characterization* 33, 87-92.
10. McPherson, N., Baker, T., and Millar, D. (1998). *Metallurgical Transactions A*. 29A, 823-832.
11. Kusko, C. (1999). MSc Thesis, Lehigh University, Bethlehem, PA.
12. Kusko, C. (1999). Unpublished research.
13. ASTM E647. (1993). *Annual Book of ASTM Standards. Section 3. Metals Test and Analytical Procedures*. 3.01, 565-601.

TABLE 1
SUBSTRATE AND FILLER METAL COMPOSITIONS

| | Fe | Ni | Cr | Mo | Nb | Si | C | P | S | Al | Ti | Mn |
|---|---|---|---|---|---|---|---|---|---|---|---|---|
| A285 | 98.31 | -- | -- | -- | -- | 0.21 | 0.06 | 0.01 | 0.028 | -- | -- | 0.81 |
| 309L | 60.33 | 12.62 | 23.44 | -- | -- | 0.40 | 0.013 | -- | -- | -- | -- | -- |

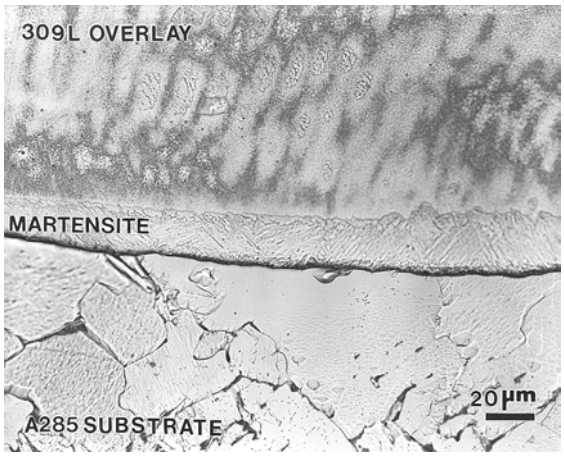


**Figure 1**. Martensite layer observed at fusion line of dissimilar metal welds (etchant: 90 ml methanol/ 5 g FeCl/ 4ml HCl, electrolytic preset at 6 volts for 3 seconds).

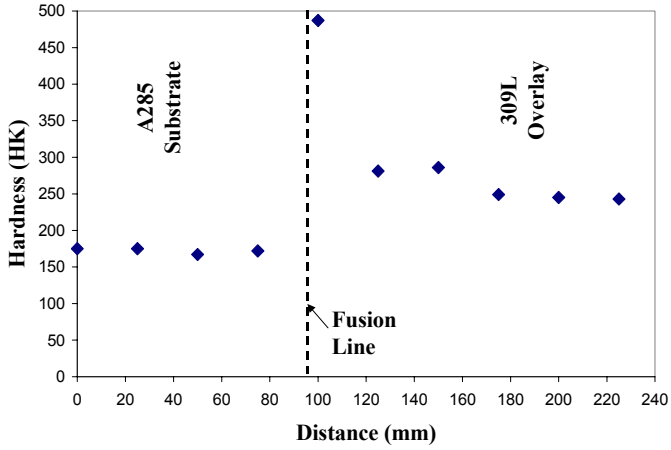


**Figure 2**. Microhardness results for 309L dissimilar weld (Knoop indenter, 10 g load for 10 seconds).

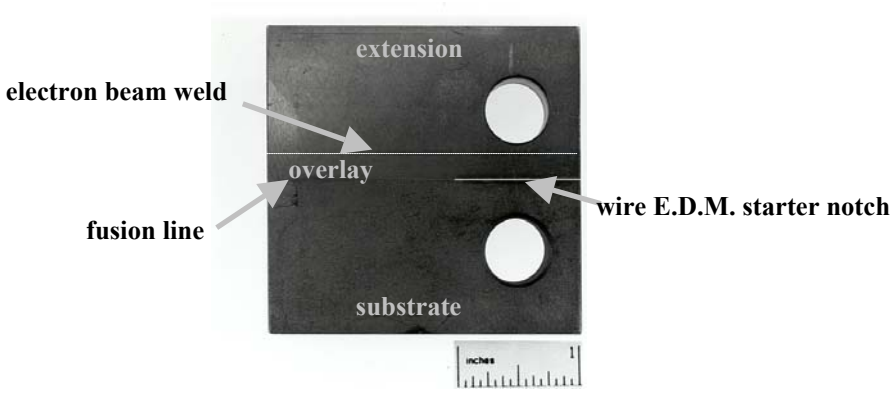


**Figure 3.** Photomacrograph illustrating typical C(T) specimen starter notch insertion.

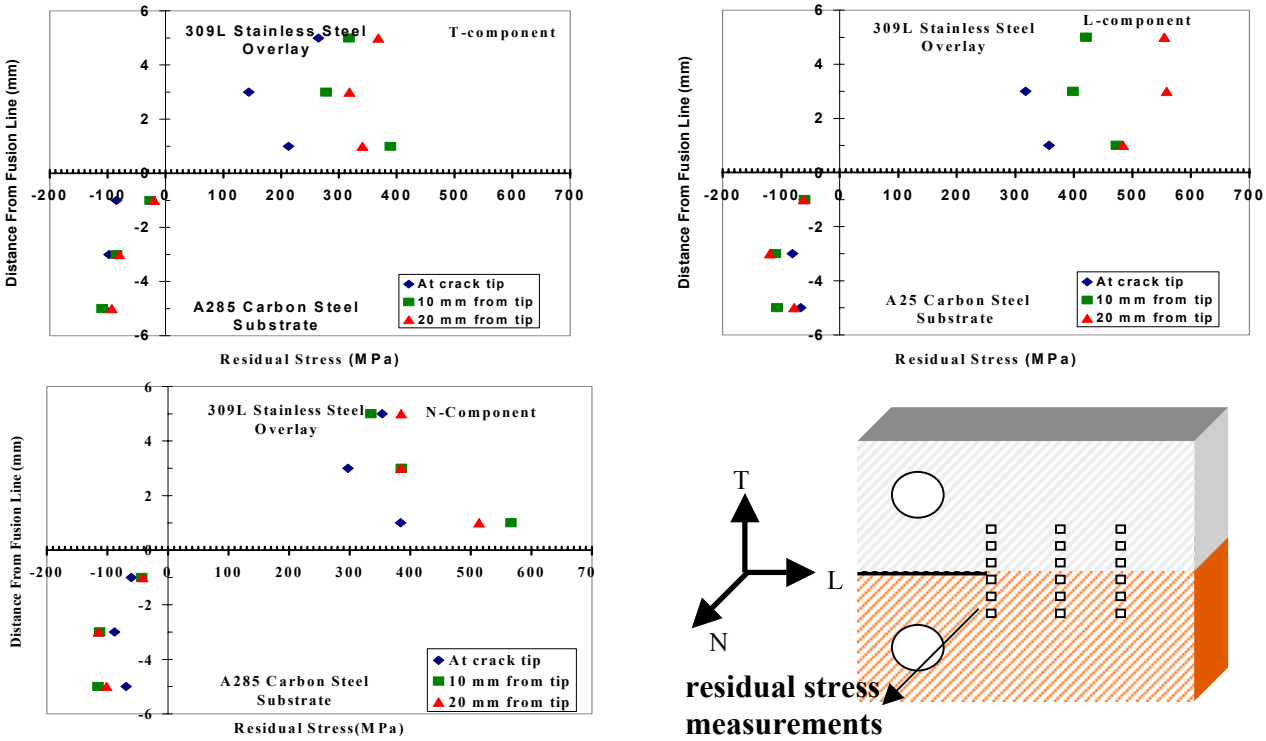


**Figure 4.** Residual stress measurements for 309L AW dissimilar metal weld specimen.

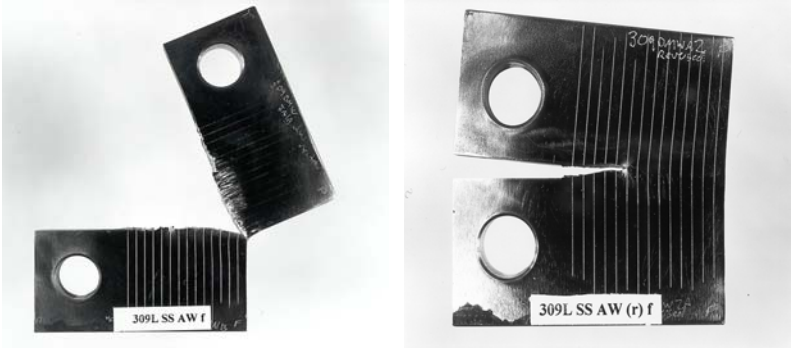


(a) (b)

**Figure 5**. Macroscopic crack growth directions for specimens a) 309DMW3 and b) 309DMW2.

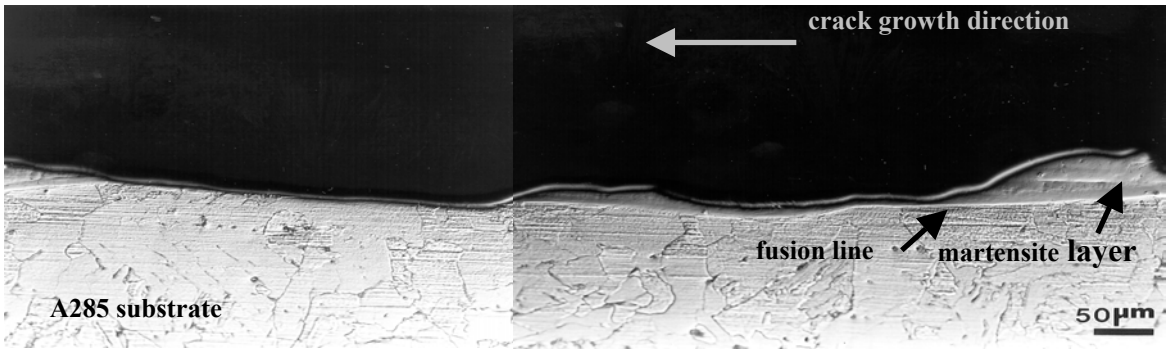


(a)

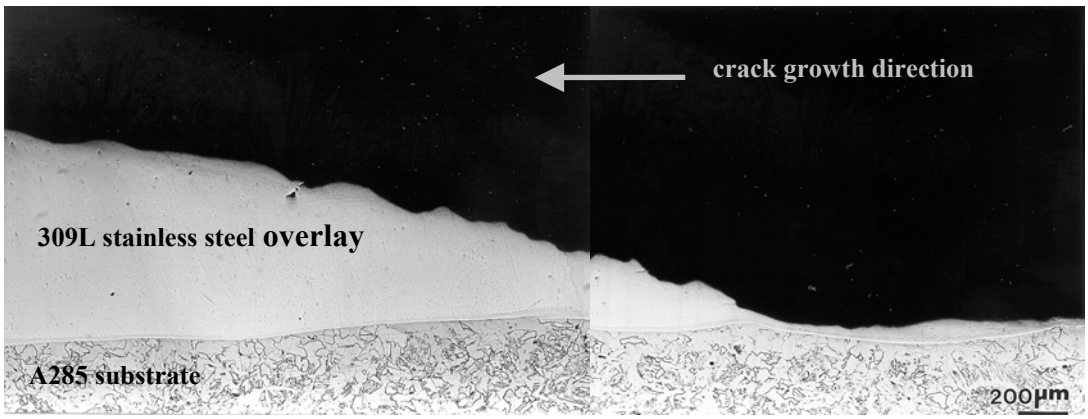


(b)

**Figure 6.** Crack growth interaction with the fusion line in 309L stainless steel dissimilar welds corresponding to test identifications 309DMW3 (AW).

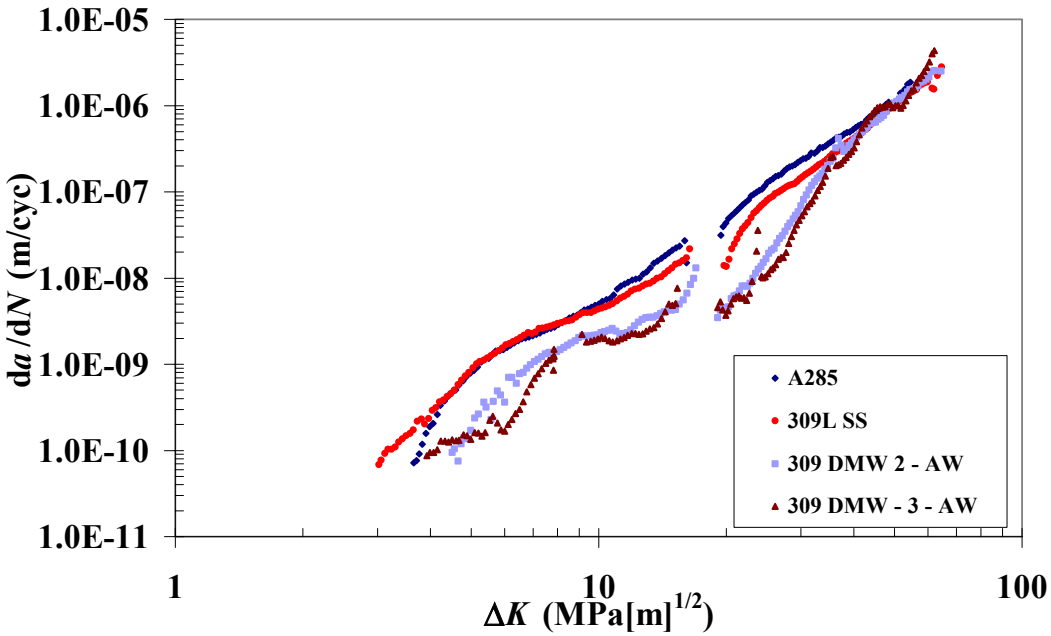


**Figure 7.** Crack growth rate curves for 309L stainless steel/A285 carbon steel dissimilar metal weld specimens and wrought A285 carbon steel and 309L stainless steel specimens.